Electrospinning of functional poly(methyl methacrylate) nanofibers containing cyclodextrin-menthol inclusion complexes

Nanotechnology **20** (2009) 125703 (10pp) doi:10.1088/0957-4484/20/12/125703

Electrospinning of functional poly(methyl methacrylate) nanofibers containing cyclodextrin-menthol inclusion complexes

Tamer Uyar[1,2,5], **Yusuf Nur**[3], **Jale Hacaloglu**[3] and **Flemming Besenbacher**[1,4]

[1] Interdisciplinary Nanoscience Center (iNANO), Aarhus University, DK-8000, Aarhus C, Denmark
[2] UNAM-Institute of Materials Science and Nanotechnology, Bilkent University, Ankara, 06800, Turkey
[3] Department of Chemistry, Middle East Technical University, Ankara, 06530, Turkey
[4] Department of Physics and Astronomy, Aarhus University, DK-8000, Aarhus C, Denmark

E-mail: tamer@inano.dk and tamer@unam.bilkent.edu.tr

Received 13 November 2008, in final form 3 February 2009
Published 4 March 2009
Online at stacks.iop.org/Nano/20/125703

Abstract

Electrospinning of nanofibers with cyclodextrin inclusion complexes (CD-ICs) is particularly attractive since distinct properties can be obtained by combining the nanofibers with specific functions of the CD-ICs. Here we report on the electrospinning of poly(methyl methacrylate) (PMMA) nanofibers containing cyclodextrin-menthol inclusion complexes (CD-menthol-ICs). These CD-menthol-IC functionalized nanofibers were developed with the purpose of producing functional nanofibers that contain fragrances/flavors with high temperature stability, and menthol was used as a model fragrance/flavor material. The PMMA nanofibers were electrospun with CD-menthol-ICs using three type of CD: α-CD, β-CD, and γ-CD. Direct pyrolysis mass spectrometry (DP-MS) studies showed that the thermal evaporation of menthol occurred over a very high and a broad temperature range (100–355 °C) for PMMA/CD-menthol-IC nanowebs, demonstrating the complexation of menthol with the CD cavity and its high temperature stability. Furthermore, as the size of CD cavity increased in the order α-CD $<$ β-CD $<$ γ-CD, the thermal evolution of menthol shifted to higher temperatures, suggesting that the strength of interaction between menthol and the CD cavity is in the order γ-CD $>$ β-CD $>$ α-CD.

(Some figures in this article are in colour only in the electronic version)

1. Introduction

Electrospinning has recently received great interest since this versatile technique enables the production of multi-functional nanofibers obtained from a wide range variety of materials including polymers, polymer blends, sol–gels, composites, and ceramics [1–3]. Electrospun nanofibers/nanowebs have a number of important characteristics such as large surface-to-volume ratio and pore sizes in the nanorange, and it is fairly easy to improve the functionality of the nanofibers by incorporating additives during the electrospinning process [4–6]. It has been shown that the remarkable properties and the multi-functionality of the nanofibers open up a number of very interesting areas of applications including areas of biotechnology, nanotechnology, and nanomedicine, and more specifically for textiles, membranes/filters, and 3D scaffolds, etc [1, 2, 7–9].

Electrospinning of nanofibers with cyclodextrins (CDs) and/or cyclodextrin inclusion complexes (CD-ICs) is of particular interest to us, since nanofibers with specific functions can be produced [10–17]. Cyclodextrins (CD) are cyclic oligosaccharides consisting of α(1,4)-linked glucopyranose units having a toroid-shaped molecular structure. The most

[5] Author to whom any correspondence should be addressed.

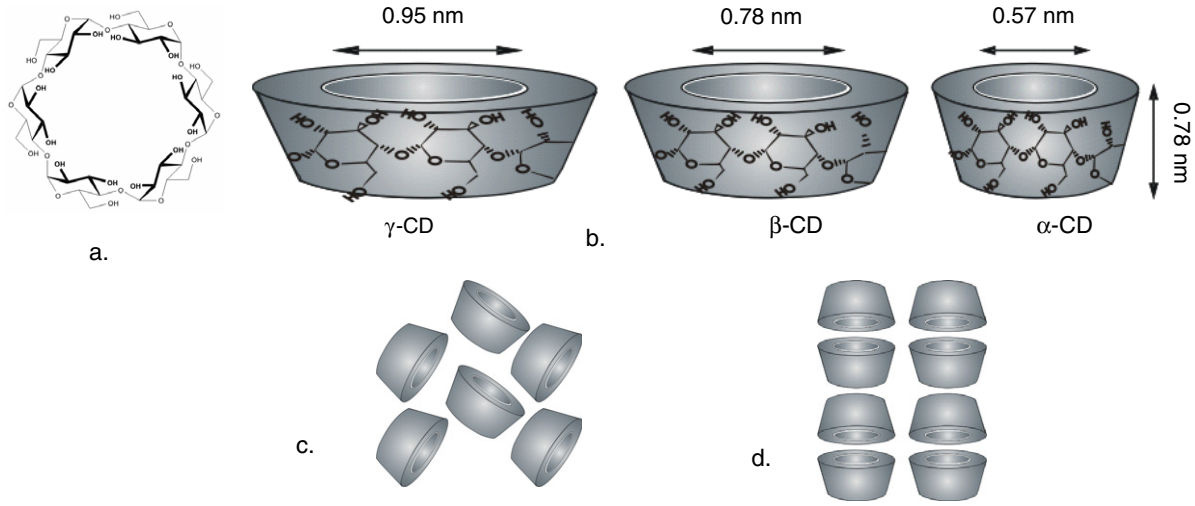

Figure 1. (a) Chemical structure of α-CD; (b) approximate dimensions of α-CD, β-CD, and γ-CD; schematic representation of packing structures of (c) cage-type and (d) channel-type CD crystals.

common natural CDs have either 6, 7, or 8 glucopyranose units in the cyclic and are referred to as α-CD, β-CD, and γ-CD, respectively (figure 1). The depth of the cavities for the three CDs is the same (∼7.8 Å), while the cavity diameters of α-CD, β-CD, and γ-CD are ∼6, 8, and 10 Å, respectively [18]. Due to the unique chemical structure of the CD molecule, the inner surface of the cavity is hydrophobic, whereas the exterior surface is hydrophilic. The hydrophobic cavity of the CDs implies that they form non-covalent host–guest complexes with various small molecules [18–21] and macromolecules [22–25]. The formation and the stability of the CD-ICs depend on many factors such as the size or shape match between host and guest, chemical environment, and the binding forces (e.g., hydrophobic interactions, van der Waals attractions, hydrogen bonding, and electrostatic interactions) between the host CD and guest molecules [21]. As the physical and chemical properties of incorporated guest compounds can be tailored by complexation with CDs, the CDs are used for the stabilization and controlled/sustained release of fragrances/flavors. Significant problems such as short shelf-life may arise due to the high volatility nature of these fragrance/flavor molecules, but it has been proven that the cyclodextrins are very effective for the stabilization of fragrance/flavor ingredients in food, cosmetics, and the textile industry [19, 20, 26–31].

The functionalization of nanofibers with cyclodextrin inclusion complexes (CD-ICs) is extremely attractive since nanowebs containing CD complexes will have unique characteristics that can potentially improve and broaden the application areas of cyclodextrins and nanofibers. Poly(methyl methacrylate) (PMMA) is a suitable fiber matrix since our previous study showed that it can be easily electrospun into uniform nanofibers with CDs without forming an inclusion complex [13], and therefore the polymer chains do not interfere with the inclusion complexation between the guest molecules and the CDs. In this study we produced functional PMMA nanofibers containing fragrances/flavors with high temperature stability. For this purpose, menthol was used as a model fragrance/flavor material and nanofibers of PMMA containing CD-menthol-ICs were electrospun by using three types of CD: α-CD, β-CD, and γ-CD. The stability and temperature release profiles of menthol for CD-menthol-IC functionalized PMMA nanofibers were investigated by direct pyrolysis mass spectrometry (DP-MS). The DP-MS results demonstrate that the stability and temperature release of menthol was sustained over a very high and a broad temperature range (100–350 °C) for all three PMMA/CD-menthol-IC nanofibers. We found that the temperature stability of menthol was the most effective in the case of PMMA/γ-CD-menthol-IC nanofibers and that the strength of interaction between menthol and the CD cavity was in the order γ-CD > β-CD > α-CD.

2. Experimental details

2.1. Materials

The poly(methyl methacrylate) (PMMA) (M_w ∼ 350 000, Aldrich), *N*,*N*-dimethylformamide (DMF) (98%, Fluka), and menthol (99%, Sigma-Aldrich) were purchased commercially. The alpha-, beta-, and gamma-cyclodextrins (α-CD, β-CD, and γ-CD) were obtained from Wacker Chemie AG, Germany. All the materials were used as received, without any further purification.

2.2. Preparation of the solutions

Menthol was dissolved in DMF and the CDs (α-CD, β-CD, and γ-CD) were added to the menthol solution, separately. The homogeneous CD-menthol mixtures were stirred for 2 h, and after that, PMMA was added to CD-menthol solutions, the temperature was raised to 60 °C, and the solutions were stirred for an additional 5 h; thereafter, the solutions were cooled down to room temperature and stirred for an additional 18 h, and then electrospun. For comparison, a PMMA/menthol solution without CD was also prepared under the same conditions, and again nanofibers were electrospun. In the

Table 1. The solution compositions and the morphological characteristics of the resulting nanofibers.

Solutions	% PMMA[a] (w/v)	%, CD type[b] (w/w)	% Menthol[b] (w/w)	Fiber diameter (nm)	Fiber morphology
PMMA/menthol	15	—	5	907 ± 91	Bead-free nanofibers
PMMA/α-CD-menthol-IC	10	31%, α-CD	5	543 ± 84	Bead-free nanofibers
PMMA/β-CD-menthol-IC	10	36%, β-CD	5	565 ± 54	Bead-free nanofibers
PMMA/γ-CD-menthol-IC	10	41%, γ-CD	5	566 ± 86	Bead-free nanofibers

[a] With respect to solvent (DMF).
[b] With respect to polymer (PMMA).

case of PMMA/CD-menthol, the PMMA concentration was kept at 10% (w/v) with respect to solvent (DMF), and for PMMA/menthol the PMMA concentration was kept 15% (w/v). The menthol content was 5% (w/w) with respect to PMMA, and the CD content was adjusted to 31% (w/w) for α-CD, 36% (w/w) for β-CD and 41% (w/w) for γ-CD, respectively, with respect to PMMA, which corresponds to the assumption that each type of CD forms a 1:1 (molar ratio) inclusion complex with menthol. The contents of the electrospun solutions are summarized in table 1.

2.3. Electrospinning

The solutions were placed in a 1 ml syringe fitted with a stainless steel metallic needle with an inner diameter of 0.4 mm. The syringe was fixed horizontally on the syringe pump (Model: KDS 101, KD Scientific) and the electrode of the high voltage power supply (Spellman High Voltage Electronics Corporation, MP Series) was clamped to the metal needle tip. The feed rate of polymer solution was 1 ml h^{-1} and the applied voltage was 15 kV. The tip-to-collector distance was set to 10 cm, and a grounded stationary rectangular metal collector (15 cm $\times$ 20 cm) covered by a piece of clean aluminum foil was used for the fiber deposition. The complete electrospinning apparatus was enclosed in a glass box, and the electrospinning of the fibers was carried out at room temperature (RT) in a horizontal position. The obtained nanowebs were dried at RT under the suction hood for 24 h to let the uncomplexed menthol evaporate and to remove any residual solvent present.

2.4. Characterization and measurements

The fiber morphologies were examined by high resolution scanning electron microscopy (SEM; FEI, Nova 600 NanoSEM and Quanta 200 FEG). The average fiber diameters were determined from the SEM images obtained, and around 50 fibers were measured. The nanofibers were annealed for 2 h at 150 °C in the oven in order to investigate their dimension stability. Two-dimensional (2D) x-ray diffraction (XRD) data of the nanowebs were collected using a Stoe Stadi P diffractometer with Cu Kα radiation over the range $2\theta = 5°$–$30°$. Some of the webs were shipped to Middle East Technical University, Turkey, for the direct pyrolysis mass spectrometry (DP-MS) analyses, and in all cases the samples were analyzed exactly 10 days after their production. The DP-MS system consists of a Waters Quattro Micro GC tandem MS with an EI ion source, and is coupled with a direct insertion probe ($T_{max} = 650$ °C). Samples (0.010 mg) were pyrolyzed in quartz sample vials at a heating rate of 10 °C min^{-1} and data can be recorded in a mass range 10–1500 Da.

3. Results and discussion

The PMMA nanofibers containing inclusion complexes (ICs) of α-CD-menthol, β-CD-menthol and γ-CD-menthol were electrospun from the common solution of PMMA, menthol, and CD (α, β, or γ) in DMF. PMMA/menthol without CD was also electrospun for comparison. In table 1 the solution compositions and the morphological characteristics of the resulting nanofibers are summarized. The SEM images of PMMA/menthol and PMMA/CD-menthol-ICs depicted in figure 2 show that the nanofibers obtained were uniform and bead-free. In terms of fiber surface morphology, we did not observe any noticeable difference between PMMA/menthol and PMMA/CD-menthol-ICs nanofibers. We also examined the dimension stability of these nanofibers by annealing at 150 °C for 2 h, and we observed that the samples kept their fibrous morphology (figure 3). The average fiber diameter (AFD) was about ~550 nm for all three PMMA/CD-menthol-IC nanowebs. For the PMMA/menthol nanoweb, the AFD was 907 $\pm$ 91 nm. The PMMA/menthol has larger AFD because 15% (w/v) PMMA was used in order to get bead-free nanofibers whereas 10% (w/v) PMMA was optimal for obtaining bead-free nanofibers from PMMA/CD-menthol-IC solutions. The addition of the CD causes an increase in the conductivity of polymer solutions, and this increase in conductivity results in bead-free electrospun nanofibers from 10% (w/v) PMMA. The positive effect of CD on electrospinning of bead-free PMMA fibers from low polymer concentrations has been discussed in detail elsewhere [13].

XRD is a useful characterization technique for investigating the crystalline structure of CDs. CDs are crystalline and have crystal structures referred to as a 'cage' or 'channel' type (figures 1(c) and (d)) [32, 33]. The commercially purchased, as-received CDs have cage structures with a 'herring-bone' arrangement in which the cavity of each molecule is blocked by neighboring molecules. For the channel structure, the CD molecules are aligned and stacked on top of each other, forming long cylindrical channels. In general, the channel arrangement of CD molecules is the confirmation for the inclusion complexation when formed with host molecules [34, 35].

The 2D XRD patterns of cage-type and channel-type packing structures of α-CD, β-CD, and γ-CD are given

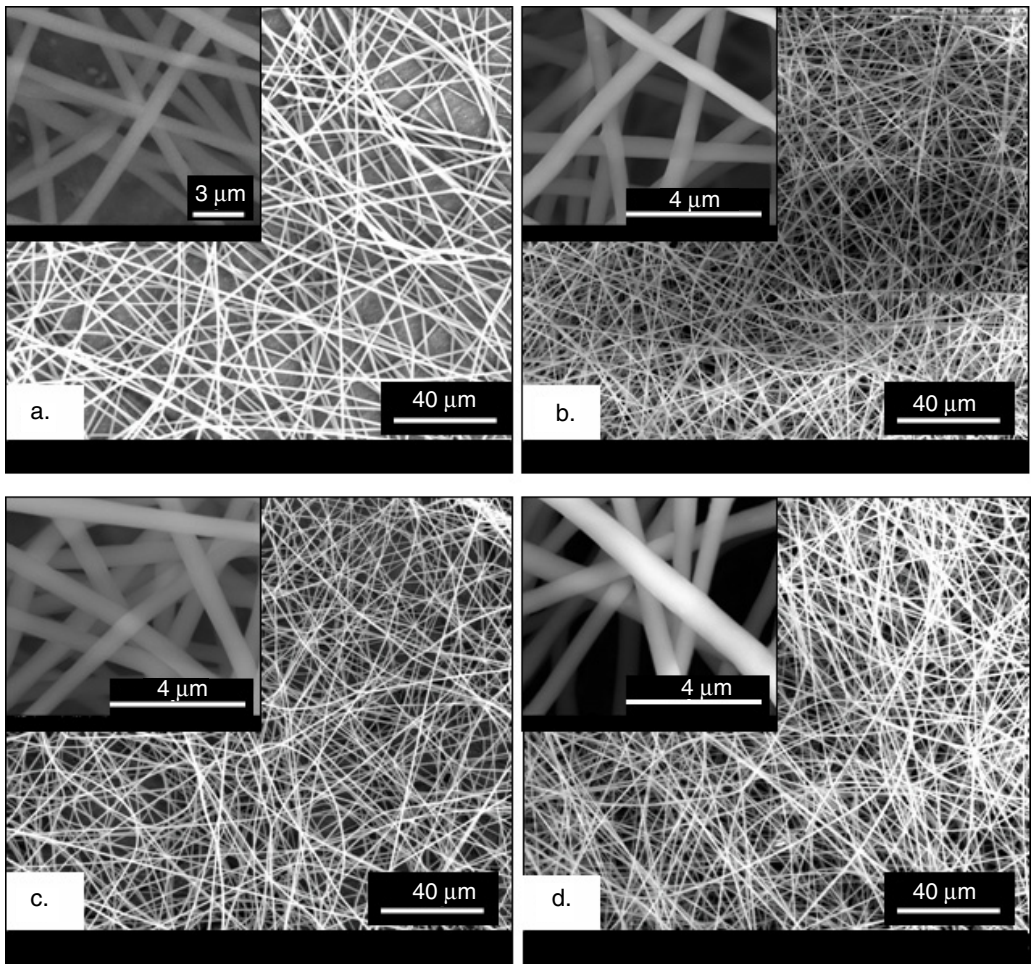

Figure 2. SEM images of electrospun nanofibers of (a) PMMA/menthol, (b) PMMA/α-CD-menthol-IC, (c) PMMA/β-CD-menthol-IC, and (d) PMMA/γ-CD-menthol-IC. The insets show higher magnification images.

in figure 4. α-CD with the channel-type packing structure has two salient peaks centered at $2\theta \cong 13°$ and 20° [36]. Channel-type γ-CD has one major peak at $2\theta \cong 7.5°$ with minor reflections at $2\theta \cong 14°$, 15°, 16°, 17° and 22° [35, 36]. The typical channel-type β-CD has major peaks at $2\theta \cong 12°$, 18°, and 19° [34].

The 2D XRD studies were performed on the pure menthol, PMMA/menthol, and PMMA/CD-menthol-IC nanowebs (figure 5). Menthol is a crystalline material having salient peaks centered at $2\theta \cong 15.6°$, 18.85° and 22°. PMMA is an amorphous polymer showing a broad halo diffraction pattern. The absence of any diffraction peak of crystalline menthol in the XRD pattern of PMMA/menthol indicated that the menthol molecules were distributed in the nanofibers without forming any crystalline aggregates. In the case of the PMMA/α-CD-menthol-ICs nanoweb, the characteristic peaks of the α-CD channel structure at $2\theta \cong 13°$ and 20° [36] were observed, confirming that α-CD-menthol-IC channel-type crystals were present in the PMMA nanofibers. For the PMMA/β-CD-menthol-IC nanoweb, very weak diffraction peaks appeared, but mostly a broad halo pattern was observed, similar to PMMA/menthol, suggesting that β-CD-menthol-IC was predominantly present in an amorphous state in the PMMA matrix. In the case of the PMMA/γ-CD-menthol-IC nanoweb, the channel-type structure of CD-IC was observed, similar to the PMMA/α-CD-menthol-IC nanoweb. The peak at $2\theta =\sim 7.5°$ is very distinct for the channel-type packing of γ-CD [35, 36] and confirms the presence of γ-CD-menthol-IC in the PMMA nanofibers. In brief, the XRD studies confirmed the incorporation of CD-menthol inclusion complexes in PMMA nanofibers for α-CD and γ-CD since CD molecules adopt channel-type packing when they form inclusion complexes [34, 35, 37]. In the case of PMMA/β-CD-menthol-IC, the XRD data did not reveal any information as to whether or not menthol was complexed with β-CD. Besides, the presence of some uncomplexed menthol buried in the nanofibers may also be possible for all the PMMA/CD-menthol systems.

The possibility of inclusion complexation between CD and PMMA [37] was also considered, but this possibility was discarded, because our previous results showed that PMMA and CD did not form a complex in the conditions and the solvent system used [13]. This further supports that the PMMA does not interfere with the inclusion complexation between menthol and the CD cavity. It is also important to mention that the complexation of CD molecules with a polymer matrix is not

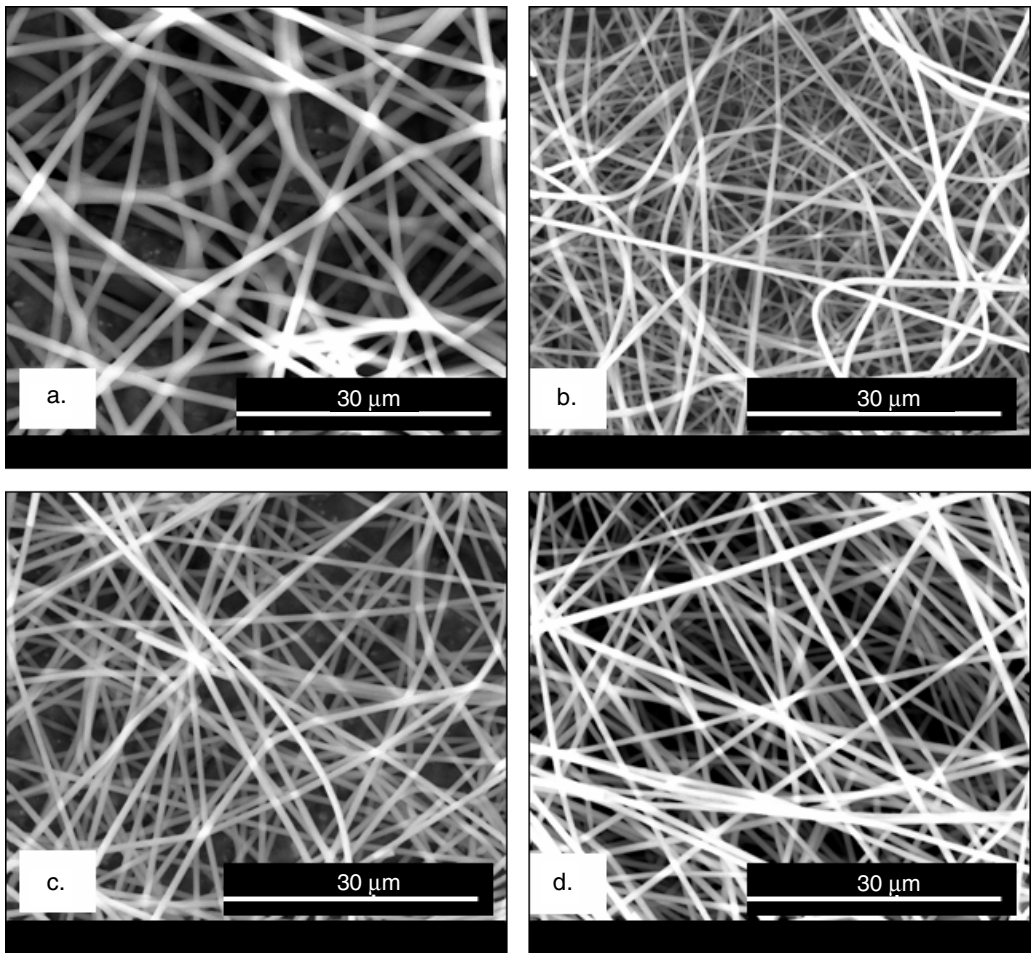

Figure 3. SEM images of electrospun nanofibers after annealing at 150 °C for 2 h: (a) PMMA/menthol, (b) PMMA/α-CD-menthol-IC, (c) PMMA/β-CD-menthol-IC, and (d) PMMA/γ-CD-menthol-IC.

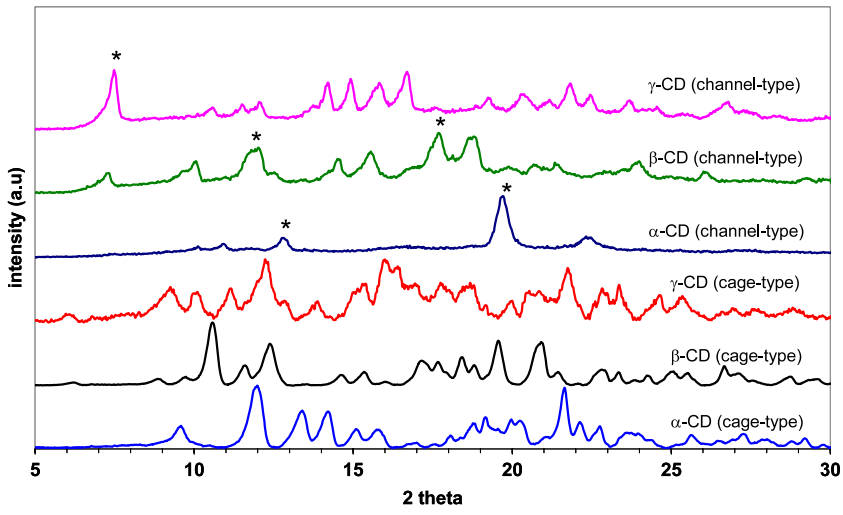

Figure 4. 2D x-ray diffraction patterns of cyclodextrins: cage-type and channel-type packing.

desired since the CD cavities would be occupied with polymer chains and therefore the CD cavities would not be available to form complexes with the additives. So the choice of polymer matrix is very important when CD functionalized nanofibers are produced by electrospinning.

The XRD technique can, however, only provide indirect information from the channel-type packing whether or not CD-menthol inclusion complex is present in the PMMA nanofibers. Therefore, we have also carried out DP-MS experiments to further explore whether the complexation of menthol with

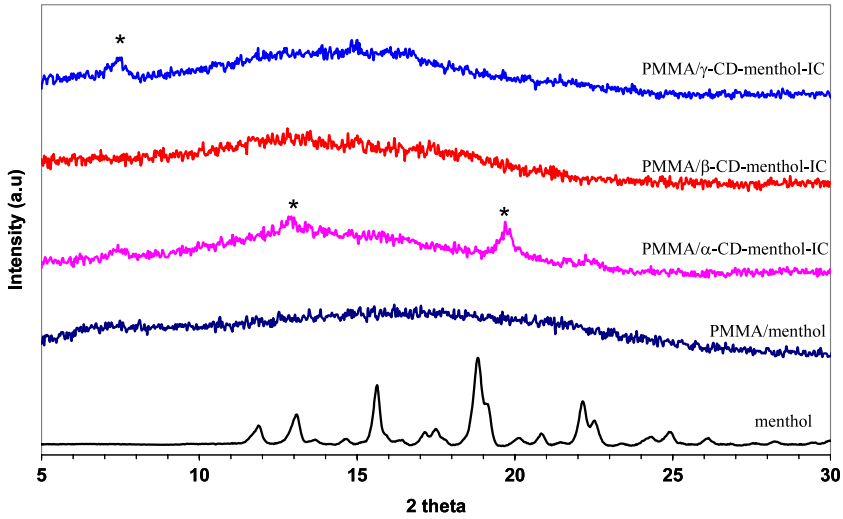

Figure 5. 2D x-ray diffraction patterns of the menthol and the nanowebs.

CDs takes place and to investigate the stability of the menthol present in the nanowebs. For a multi-component system, DP-MS allows the separation of components as a function of their volatilities and/or thermal stabilities. Once included in the host CD cavities, the thermal evaporation of the volatile guest molecules shifts to higher temperatures due to the strong interaction with the CD cavity, and DP-MS is a very useful technique to characterize the CD host–guest inclusion complexes [38].

By means of the DP-MS technique we can analyze thermal characteristics such as volatility, thermal stability, and degradation products of the materials [39, 40]. However, pyrolysis mass spectra of a multi-component system, especially those involving polymers, are usually very complex due to the dissociative ionization processes and due to the fact that all fragments with the same mass to charge ratio contribute to the intensity of the same peak in the mass spectrum. Thus, in pyrolysis MS analysis, not only the detection of the product, but also the variation of its yield as a function of temperature, i.e. the thermal evolution profile, is very important in order to determine the source of the product.

To investigate the presence of menthol and evaluate its thermal stability in the nanowebs, the DP-MS analysis of pure menthol was carried out for comparison. Under the high vacuum conditions of MS, the immediate evolution of menthol was in accordance with very volatile flavor/fragrance material characteristics of menthol. The product yield was maximized in 0.70 min (around room temperature) and decreased steadily and then totally disappeared. In figure 6, the total ion current (TIC; variation of total ion yield as a function of temperature) curve and the pyrolysis mass spectrum recorded at 0.70 min are depicted. The recorded pyrolysis mass spectrum, involving a base peak at $m/z = 71$ Da, intense peaks at $m/z = 81$, 95, 123, and 138 Da, and a very weak molecular ion peak at $m/z = 156$ Da, is identical to the mass spectrum of menthol given in mass libraries, confirming the evaporation of menthol.

On the other hand, the TIC curves of PMMA/CD-menthol-IC nanofibers showed two peaks: a weak one with a maximum around 160 °C and a broad and intense one with a maximum around 400 °C. In figure 6, the TIC curve and the mass spectra recorded at the peak maxima present in the TIC curve detected during the pyrolysis of PMMA/α-CD-menthol-IC are depicted as an example. The similarity between the mass spectra recorded around 160 °C (figure 7(b)) and the mass spectrum of menthol (figure 6(b)) confirms the evolution of menthol in this temperature region. It is known that PMMA degrades via depolymerization, resulting mainly in the monomer MMA [41]. The pyrolysis mass spectra detected at around 400 °C show the typical fragmentation pattern of MMA, with intense peaks at $m/z = 100$, 69, and 41 Da due to molecular ions of MMA and $CH_2 = C(CH_3)CO$ and $CH_2 = CCH_3$, respectively. This confirms the depolymerization of PMMA in accordance with the existing literature results [41]. On the other hand, the characteristic peaks for the CD at 60 and 73 Da present in the pyrolysis mass spectra recorded at around 360 °C are due to $C_2H_4O_2$ and $C_3H_5O_2$ fragments.

In figure 8, the evolution profiles of some characteristic fragment ions of each component, namely 138, 60, and 100 Da ions due to fragment ions generated by the loss of H_2O from menthol, $C_2H_4O_2$ ions of CD, and molecular ions of MMA, respectively, are shown for PMMA/menthol and PMMA/CD-menthol-IC nanowebs. To our surprise, the PMMA/menthol nanofibers without CD show release of menthol at higher temperatures compared to the situation for pure menthol. The retention of menthol at high temperature in PMMA nanofibers may be due to the strong interactions such as hydrogen bonding between menthol molecules and PMMA chains. Unlike PMMA, we have recently shown that electrospun polystyrene (PS) fibers could not preserve volatile menthol molecules at high temperatures without the CD inclusion complexes [15].

When we compare PMMA/menthol and PMMA/CD-menthol-IC nanofibers for the temperatures at which menthol evolution was maximized, a noticeable shift to high temperature ranges was observed for the PMMA/CD-menthol-IC. The peak maxima in the TIC evolution profiles of menthol for PMMA/menthol and PMMA/α-CD-menthol-IC

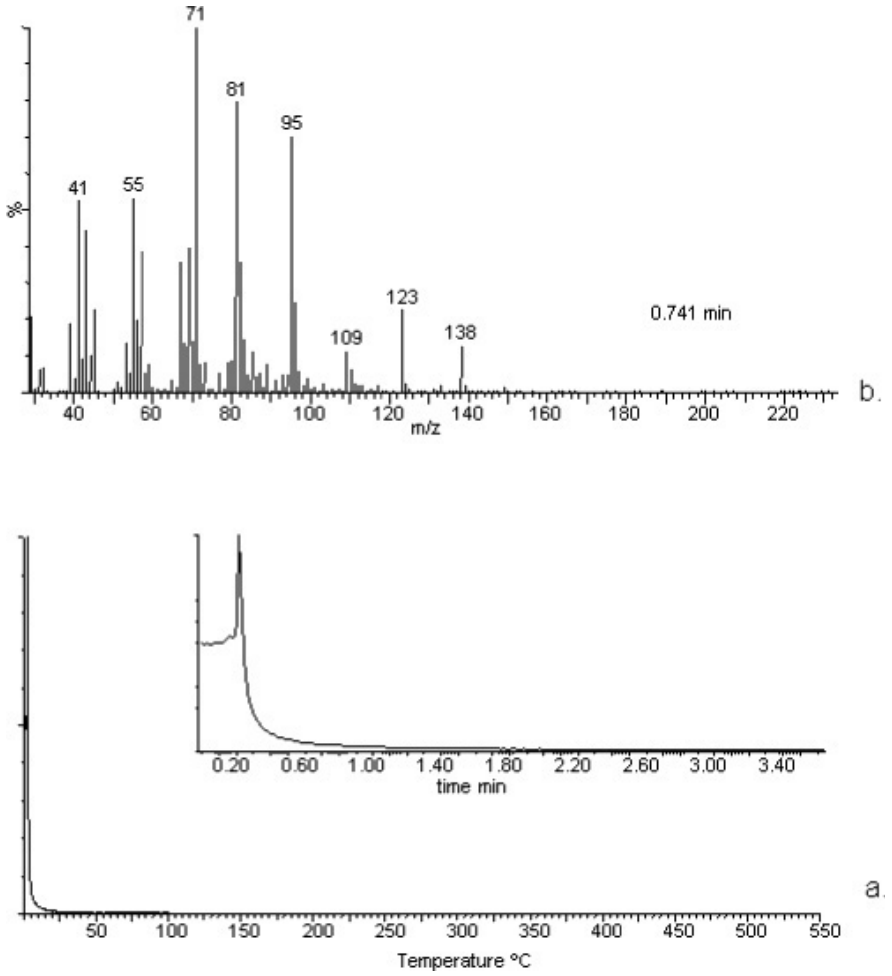

Figure 6. (a) The TIC curve and (b) the pyrolysis mass spectrum recorded for pure menthol.

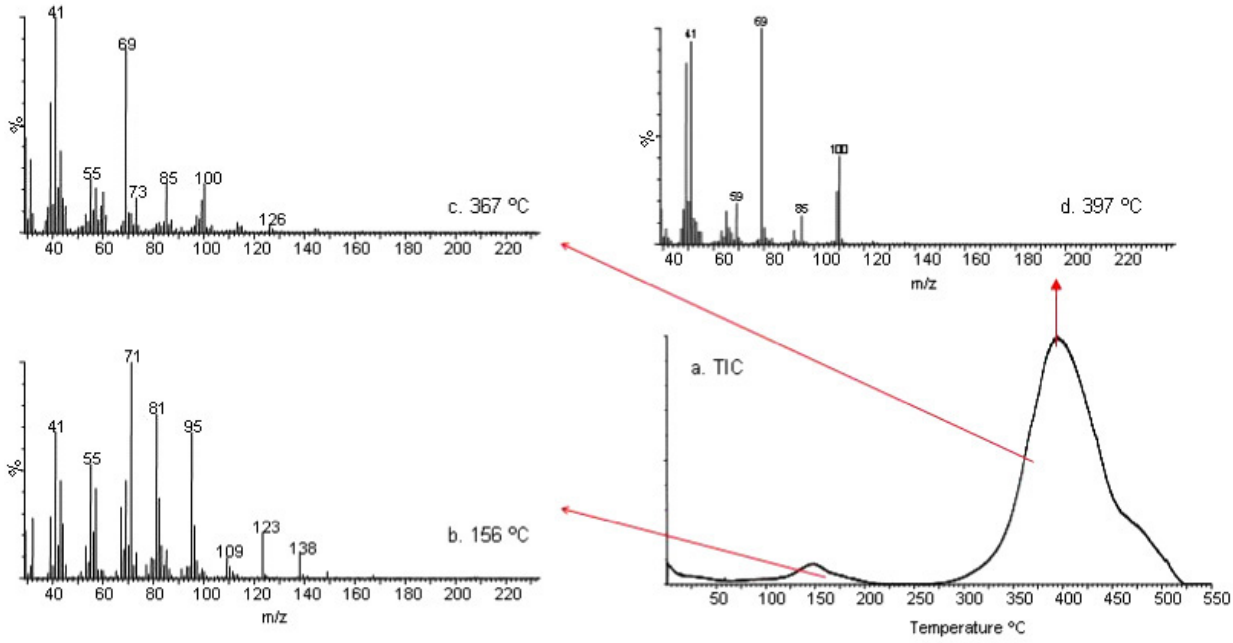

Figure 7. The TIC curve and the mass spectra recorded at the peak maxima present in the TIC curve detected during the pyrolysis of PMMA/α-CD-menthol-IC.

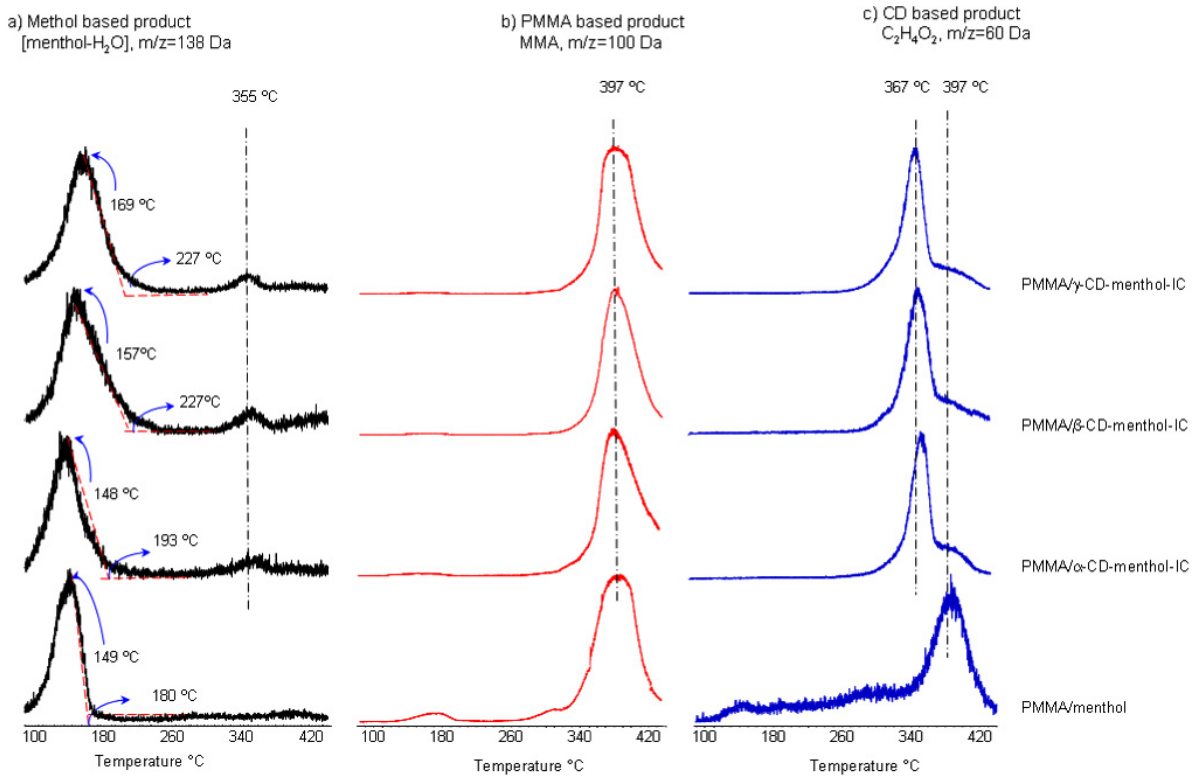

Figure 8. Evolution profiles of some characteristic fragment ions of each component, namely 138, 60, and 100 Da ions due to loss of H_2O from menthol, $C_2H_4O_2$ ions from CD, and molecular ions for MMA.

were almost the same, and they appeared at around 150 °C. However, for the nanofibers containing β-CD and γ-CD, the peak maximum temperature for menthol was observed to occur at around 160 °C and 170 °C, respectively. Furthermore, as the size of the CD increased in the order $\alpha < \beta < \gamma$, the broadening in the TIC release profiles of menthol based products also increased. The PMMA/menthol nanofibers without CD have also shown release of menthol at higher temperatures; however, it was observed that the thermal evaporation of menthol occurred over a higher and a broader temperature range for the PMMA/CD-menthol-IC nanowebs. This finding confirmed that the menthol was complexed with the CD cavity and its temperature stability was increased. Furthermore, in the evolution profiles of menthol based products for PMMA/CD-menthol-IC nanowebs, a weak and broad peak with a maximum around 355 °C was recorded. However, this temperature is very close to 367 °C at which the maximum is present in the evolution profiles of CD based products, but the difference was reproducible and statistically significant. For a better understanding, the trends in the temperature release profiles of menthol and CD based products detected during the pyrolysis of PMMA/γ-CD-menthol-IC are shown in figure 9 for the temperature range 300–420 °C. Thus, we tentatively suggest that a stronger interaction, most probably hydrogen bonding, between menthol and CD also exists for the complex and sustained the release of some quantity of menthol at very high temperatures.

In summary, the DP-MS data indicate that, for the PMMA/α-CD-menthol-IC nanoweb, the interaction between α-CD and menthol is negligible, but the evolution of menthol occurred over a broader temperature range when compared to the release for the PMMA/menthol nanoweb. However, stronger interactions exist between the menthol and β-CD and γ-CD, the interaction being strongest for γ-CD. This finding is consistent with the previous findings in the literature where stronger interaction was reported for γ-CD and menthol complexes when compared to β-CD [31]. Thus, the DP-MS results indeed confirm the presence of CD-menthol-ICs in PMMA nanowebs, and the findings clearly reveal the stability and sustained release of menthol in higher temperature ranges (100–355 °C). Furthermore, the presence of menthol and its high temperature release profiles, as observed by the DP-MS technique even 10 days after the production of nanofibers, strongly suggest that these PMMA/CD-menthol-IC nanowebs may have attractive applications for the stabilization and sustained release of volatile fragrances/flavors in general.

4. Conclusion

Cyclodextrin-menthol inclusion complexes (CD-menthol-ICs) were successfully incorporated in poly(methyl methacrylate) (PMMA) nanofibers using and electrospinning technique for the purpose of developing functional nanofibers. PMMA/CD-menthol-IC nanowebs were obtained by using three types of CD: α-CD, β-CD, and γ-CD. Despite the high volatility of menthol, it was observed that the thermal evaporation of menthol occurred over at very high and broad temperature range (100–355 °C) for PMMA/CD-menthol-IC nanowebs. This finding confirmed the presence of the CD-menthol complex in the PMMA nanofibers; therefore, the stability

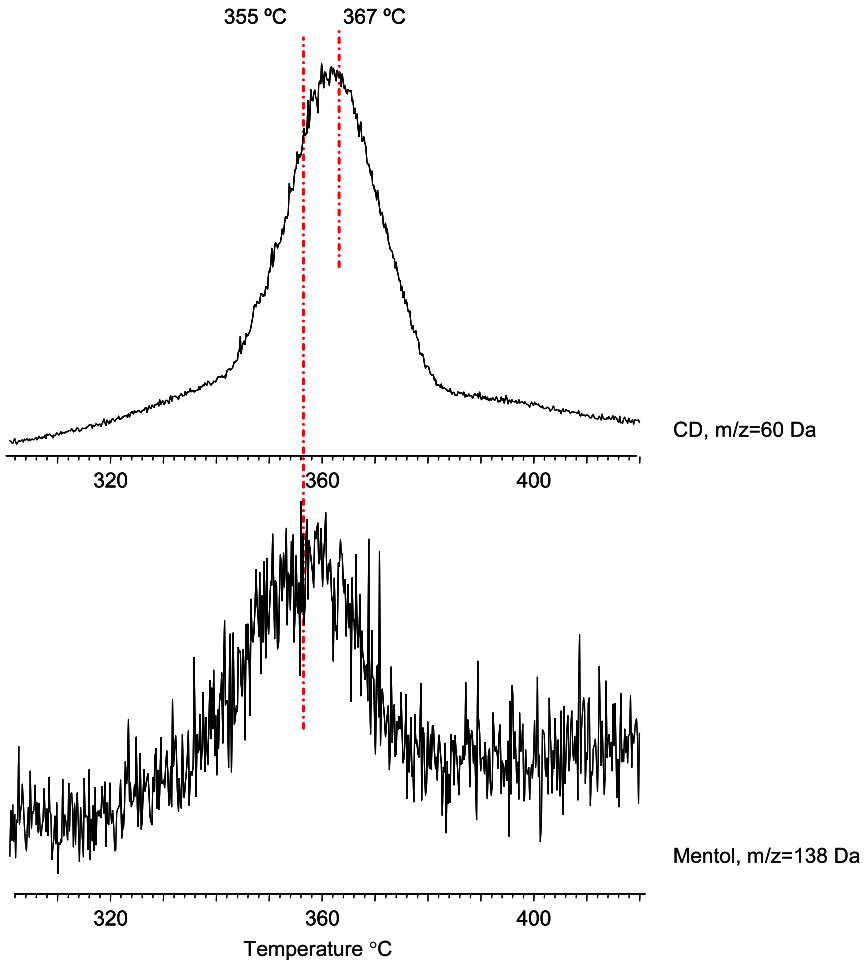

Figure 9. The trends in the evolution profiles of menthol and CD based products detected during the pyrolysis of PMMA-γ-CD-menthol-IC in the higher temperature range.

and sustained release of menthol was achieved at elevated temperatures. The thermal evolution profiles of menthol shifted to higher temperatures for PMMA/CD-menthol-IC nanowebs in the order of γ-CD > β-CD > α-CD, suggesting that the strength of interaction between menthol and the CD cavity is strongest for γ-CD. In summary, we showed that nanofibers functionalized with cyclodextrin inclusion complexes (CD-ICs) can be produced by an electrospinning technique and that these CD-IC functionalized nanofibers will be very practical for the development of functional textile materials since they show high temperature stability for volatile fragrances/flavors.

Acknowledgments

We gratefully acknowledge the funding to the current project NanoNonwovens from The Danish Advanced Technology Foundation, the collaboration with Fibertex A/S, and the Danish Research Agency for the funding to the iNANO center.

References

[1] Greiner A and Wendorff J H 2007 *Angew. Chem. Int. Edn* **46** 5670–703
[2] Li D and Xia Y 2004 *Adv. Mater.* **16** 1151–70
[3] Teo W E and Ramakrishna S 2006 *Nanotechnology* **17** R89–106
[4] Roso M, Sundarrajan S, Pliszka D, Ramakrishna S and Modesti M 2008 *Nanotechnology* **19** 285707
[5] Jin W J, Lee H K, Jeong E H, Park W H and Youk J H 2005 *Macromol. Rapid Commun.* **26** 1903–07
[6] Sikareepaisan P, Suksamrarn A and Supaphol P 2008 *Nanotechnology* **19** 015102
[7] Pham Q P, Sharma U and Mikos A G 2006 *Tissue Eng.* **12** 1197–211
[8] Burger C, Hsiao B S and Chu B 2006 *Annu. Rev. Mater. Res.* **36** 333–68
[9] Barhate R S and Ramakrishna S 2007 *J. Membr. Sci.* **296** 1–8
[10] Ramaseshan R, Sundarrajan S, Liu Y J, Barhate R S, Lala N L and Ramakrishna S 2006 *Nanotechnology* **17** 2947–53
[11] Kaur S, Kotaki M, Ma Z, Gopal R and Ramakrishna S 2006 *Int. J. Nanosci.* **5** 1–11
[12] Uyar T, Kingshott P and Besenbacher F 2008 *Angew. Chem. Int. Edn* **47** 9108–11
[13] Uyar T, Balan B, Toppare L and Besenbacher F 2008 *Polymer* **50** 475–80
[14] Uyar T and Besenbacher F 2009 *Eur. Polym. J.* at press doi:10.1016/j.eurpolymj.2008.12.024
[15] Uyar T, Hacaloglu J and Besenbacher F 2009 *Reactive and Functional Polymers* at press doi:10.1016/j.reactfunctpolym.2008.12.012
[16] Uyar T, Havelund R, Hacaloglu J, Zhou X, Besenbacher F and Kingshott P 2009 *Nanotechnology* at press
[17] Uyar T, Havelund R, Nur Y, Hacaloglu J, Besenbacher F and Kingshott P 2009 *J. Membr. Sci.* at press doi:10.1016/j.memsci.2009.01.047

[18] Szejtli J 1998 *Chem. Rev.* **98** 1743–53
[19] Hedges A R 1998 *Chem. Rev.* **98** 2035–44
[20] Del Valle E M M 2004 *Process Biochem.* **39** 1033–46
[21] Rekharsky M V and Inoue Y 1998 *Chem. Rev.* **98** 1875–917
[22] Harada A 2001 *Acc. Chem. Res.* **34** 456–64
[23] Wenz G, Han B-H and Muller A 2006 *Chem. Rev.* **106** 782–817
[24] Frampton M J and Anderson H L 2007 *Angew. Chem. Int. Edn* **46** 1028–64
[25] Uyar T, Rusa C C, Wang X, Rusa M, Hacaloglu J and Tonelli A E 2005 *J. Polym. Sci.* B **43** 2578–93
[26] Szejtli J 2003 *Starch-Starke* **55** 191–6
[27] Buschmann H J, Knittel D and Schollmeyer E 2001 *J. Incl. Phenom. Macrocycl. Chem.* **40** 169–72
[28] Liu X D, Furuta T, Yoshii H, Linko P and Coumans W J 2000 *Biosci. Biotech. Biochem.* **64** 1608–13
[29] Reineccius T A, Reineccius G A and Peppard T L 2003 *J. Food Sci.* **68** 1234–9
[30] Layre A M, Gosselet N M, Renard E, Sebille B and Amiel C 2002 *J. Incl. Phenom. Macrocycl. Chem.* **43** 311–7
[31] Yoshii H, Sakane A, Kawamura D, Neoh T L, Kajiwara H and Furuta T 2007 *J. Incl. Phenom. Macrocycl. Chem.* **57** 591–6
[32] Saenger W, Jacob J, Gessler K, Steiner T, Hoffmann D, Sanbe H, Koizumi K, Smith S M and Takaha T 1998 *Chem. Rev.* **98** 1787–802
[33] Harata K 1998 *Chem. Rev.* **98** 1803–27
[34] Harada A, Okada M, Li J and Kamachi M 1995 *Macromolecules* **28** 8406–11
[35] Uyar T, Hunt M A, Gracz H S and Tonelli A E 2006 *Cryst. Growth Des.* **6** 1113–9
[36] Rusa C C, Bullions T A, Fox J, Porbeni F E, Wang X and Tonelli A E 2002 *Langmuir* **18** 10016–23
[37] Uyar T, Rusa C C, Hunt M A, Aslan E, Hacaloglu J and Tonelli A E 2005 *Polymer* **46** 4762–75
[38] Uyar T, El-Shafei A, Wang X, Hacaloglu J and Tonelli A E 2006 *J. Incl. Phenom. Macrocycl. Chem.* **55** 109–21
[39] Uyar T, Aslan E, Tonelli A E and Hacaloglu J 2006 *Polym. Degrad. Stab.* **91** 1–11
[40] Uyar T, Rusa C C, Tonelli A E and Hacaloglu J 2007 *Polym. Degrad. Stab.* **92** 32–43
[41] Ferriol M, Gentilhomme A, Cochez M, Oget N and Mieloszynski J L 2003 *Polym. Degrad. Stab.* **79** 271–81